OH^- versus SH^- Nucleophilic Attack on Amides: Dramatically Different Gas-Phase and Solvation Energetics

Allison E. Howard and Peter A. Kollman*

Contribution from the Department of Pharmaceutical Chemistry, University of California—San Francisco, San Francisco, California 94143.
Received December 4, 1986

Abstract: The gas- and solution-phase reaction energetics for the nucleophilic addition of the hydrosulfide anion to formamide have been explored by ab initio and molecular mechanical methods. An ion–dipole complex has been identified on the gas-phase reaction coordinate, but no stable tetrahedral complex was found. Solvation stabilizes both the reactants and the addition complex; however, the solvation of the reactants is significantly less than previous workers have calculated for the analogous reaction with a hydroxide nucleophile. These results have been compared with calculated HO^-/H_2NCHO, HO^-/H_2CO, and HS^-/H_2CO nucleophilic interactions.

Nucleophilic displacement reactions at carbonyl centers are important processes in organic chemistry and biochemistry and have been the focus of considerable experimental and theoretical research. It is generally thought[1] that the reaction mechanism involves attack of a nucleophile on the polarized carbonyl group leading to the formation of a tetrahedral intermediate (Scheme I). The tetrahedral intermediate may subsequently decompose to yield the products. For many years, experimental efforts at studying these reactions in the solution phase have provided abundant support for the presence of tetrahedral intermediates. It has been possible recently to study the intermediates themselves by ultraviolet and nuclear magnetic resonance spectroscopy.[2]

In gas-phase investigations[3] of nucleophilic addition to carbonyl compounds, evidence for the tetrahedral intermediate is more equivocal than in the solution phase. In particular, the nature of the tetrahedral species has been questioned.[4] Asubiojo and Brauman[4] have concluded from ion cyclotron resonance spectroscopy experiments, utilizing a variety of nucleophiles and acyl halide substrates, that the gas-phase mechanism involves a tetrahedral transition state and not a tetrahedral intermediate. They visualize the reaction coordinate as containing two minima which correspond to ion–dipole complexes of the nucleophile and reactant or product. The superposition of these two minima on the energetically less favorable addition complex potential results in a saddle point rather than the intermediate seen in solution studies. Their conclusion is consistent with experimental gas-phase rate and product ratio data,[3,4] which show the reaction to be considerably slower than the collision frequencies and the products to be more numerous than one would predict from a tetrahedral intermediate.

A number of groups[1c,5-7] have studied nucleophilic attack of simple anions on formaldehyde and other carbonyl substrates and have found no barrier to the attack. However, when Yamabe and Minato[8a] calculated the ab initio reaction path for halide attack

Scheme I

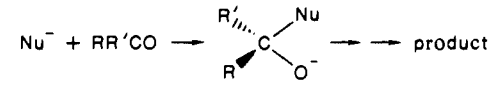

Scheme II

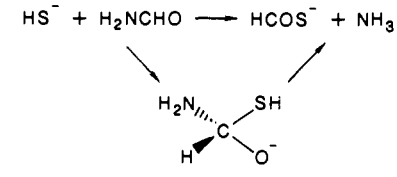

on acetyl chloride, they did not find a stable tetrahedral intermediate. Instead, reactions with both fluoride and chloride anions showed double-well potential profiles indicative of the ion–dipole complexes. The potential wells were much more pronounced for the chloride case. More recently, Blake and Jorgensen[8b] repeated the calculation of chloride ion nucleophilic attack on acetyl chloride at a higher computational level and extended the work to the chloride ion–formyl chloride reaction. They[8b] similarly found double-well energy surfaces with the tetrahedral species identified as a transition state rather than an reaction intermediate.

Weiner, Singh, and Kollman[9] have used a combined quantum mechanical/molecular mechanical approach to study the gas- and solution-phase energy profiles of the hydroxide–formamide nucleophilic reaction. A gas-phase reaction coordinate for hydroxide anion attack perpendicular to the amide plane was explored by ab initio quantum mechanics and was found to contain no potential barrier to the formation of a tetrahedral adduct. Their most sophisticated ab initio model showed the adduct to be stabilized by a enthalpy of 26.3 kcal mol^{-1} relative to the reactants. Weiner et al.[9] did not describe in detail possible ion–dipole complexes because unrestrained geometry optimization led to an alternative gas-phase reaction whereby the hydroxide ion abstracted an amide proton to form the resonance-stabilized formamide anion and water. Using molecular mechanical methods to analyze H_2O–solute interactions, Weiner et al.[9] found a barrier of 21.7 kcal mol^{-1} to the formation of the tetrahedral adduct in solution. The adduct itself was calculated to be 16.0 kcal mol^{-1} less stable than the reactants.

The gas- and solution-phase energetics for the reaction of hydroxide with formaldehyde have been recently carried out by Madura and Jorgensen[10] using ab initio and Monte Carlo methods. The most stable entity on the gas-phase reaction path was the

(1) (a) Harris, J. M.; Wamser, C. C. *Fundamentals of Organic Reaction Mechanisms*; Wiley: New York, 1976; Chapter 5. (b) Patai, S., Ed. *The Chemistry of the Carbonyl Group*; Interscience: New York, 1976. (c) Csizmadia, I. G.; Peterson, M. R.; Kozmutza, C.; Robb, M. A. In *The Chemistry of Acid Derivatives*, Part 1, Suppl. B; Patai, S., Ed.; Wiley: New York, 1979, Chapter 1. (d) Cockerill, A. F.; Harrison, R. G. *The Chemistry of Double-Bonded Functional Groups*, Part 1, Suppl. A; Patai, S., Ed.; Wiley: New York, 1977; Chapter 4.

(2) Capon, B.; Dosunmu, M. I.; Sanchez, M. *Adv. Phys. Org. Chem.* **1985**, *21*, 37.

(3) For a recent review, see: Riveros, J. M.; José, S. M.; Takashima, K. *Adv. Phys. Org. Chem.* **1985**, *21*, 197.

(4) Asubiojo, O. I.; Brauman, J. I. *J. Am. Chem. Soc.* **1979**, *101*, 3715.

(5) Bürgi, H. B.; Lehn, J. M.; Wipff, G. *J. Am. Chem. Soc.* **1974**, *96*, 1956.

(6) Stone, A. J.; Erskine, R. W. *J. Am. Chem. Soc.* **1980**, *102*, 7185.

(7) (a) Williams, I. H.; Maggiora, G. M.; Schowen, R. L. *J. Am. Chem. Soc.* **1980**, *102*, 7831. (b) Scheiner, S.; Lipscomb, W. N.; Kleier, D. A. *J. Am. Chem. Soc.* **1976**, *98*, 4770. (c) Sheldon, J. C. *Aust. J. Chem.* **1981**, *34*, 1189. (d) Alagona, G.; Scrocco, E.; Tomasi, J. *J. Am. Chem. Soc.* **1975**, *97*, 6976.

(8) (a) Yamabe, S.; Minato, T. *J. Org. Chem.* **1983**, *48*, 2972. (b) Blake, J. F.; Jorgensen, W. L. *J. Am. Chem. Soc.* **1987**, *100*, 3861.

(9) Weiner, S. J.; Singh, U. C.; Kollman, P. A. *J. Am. Chem. Soc.* **1985**, *107*, 2219.

(10) Madura, J. D.; Jorgensen, W. L. *J. Am. Chem. Soc.* **1986**, *108*, 2517.

0002-7863/88/1510-7195$01.50/0

tetrahedral adduct, which was found to be a true energy minimum. Furthermore, a small barrier existed between the tetrahedral intermediate and the ion–dipole complex of the hydroxide anion and formaldehyde. Thus, a multiple-well potential may exist for this reaction, but the energy minimum appears to be the tetrahedral intermediate. The solution studies of Madura and Jorgensen,[10] using Monte Carlo methods, are qualitatively similar to that found for the hydroxide–formamide system.[9]

In this paper, we report our results of a theoretical investigation of hydrosulfide nucleophilic displacement on formamide (Scheme II). Our interest in the hydrosulfide ion stems from its position as a third row analogue to the hydroxide ion and the possible implications of this work to the mechanism of thiol protease amide hydrolysis. During the investigation, we examined the gas-phase reaction coordinate for nucleophilic attack on the forementioned carbonyl compound and also studied the effects of solvation on two supermolecular configurations along the hydrosulfide–formamide reaction path. In addition, we studied a quantum mechanical reaction path for hydrosulfide attack on formaldehyde. Our methods parallel those used[9] in a study of hydroxide–formamide gas- and solvent-phase reaction paths.

Computational Methods

Ab Initio Energy Minimizations and Reaction Coordinates. The gas-phase nucleophilic reactions of hydrosulfide and hydroxide anions with formaldehyde and formamide were probed with the GAUSSIAN 82 program.[11] The initial experimental geometries[12] of the reactants and products shown in Scheme II were optimized, without constraints, at several ab initio levels. Single-point calculations were then carried out on the individual reactant and product molecules in order to evaluate the basis set and correlation energy dependence of the reaction energetics. The results of these calculations are shown in Table I. The two additional reactions depicted in eq 1 and 2 were also investigated by the above

$$HS^- + H^+ \rightarrow H_2S \quad (1)$$

$$HCOS^- + H^+ \rightarrow HCOSH \quad (2)$$

methodology. The proton affinities thus obtained (Table I) were used to further evaluate the performance of each quantum mechanical model.

Experimental data, from which one may test the various quantum mechanical models, exist for the proton affinity of hydrosulfide. A proton affinity value of 353.4 kcal mol^{-1} has been obtained by Bartmess and McIver.[13] Thus, most of our models overestimate the proton affinity by $\sim$10 kcal mol^{-1}. The proton affinity of thioformic acid anion has not been measured to the best of our knowledge. We would expect it to be similar to that of the formic acid anion, which was found[14] to be 342 kcal mol^{-1}. If this expectation is valid, then the split-valence models would again be within 10 kcal mol^{-1} of the actual proton affinity.

The split-valence quantum mechanical calculations predict the reaction of Scheme II to be isothermal or slightly exothermic. Because of the relative dearth of experimental data with which to compare our results, we choose to proceed with the study utilizing 4-31G optimized structures with single-point calculations at the FMP2-FC/6-31G* level. This choice provided us with three energies for each step of the reaction: 4-31G, 6-31G*, and FMP2-FC/6-31G*; allowing some internal verification of the calculational consistency. All degrees of freedom were relaxed during the calculations except the distance between the sulfur and carbon atoms.

The gas-phase reaction profiles for hydroxide and hydrosulfide nucleophilic addition to formaldehyde were also examined. These calculations were carried out as described above with the distinction that all geometry optimizations and single-point calculations were made at the 4-31G level.

Solvation Calculations. The solvent studies were accomplished with the molecular mechanics program AMBER.[15] Two supermolecular complexes were scrutinized: one having a sulfur–carbon distance of 2 Å and the other with a distance of 6 Å. The former structure was chosen because of its presumed resemblance to the activated complex for the gas-phase reaction coordinate, which we studied, while the latter approximates the separated reactant molecules. Both complexes had previously undergone geometry optimization using GAUSSIAN 82.[11] The complexes were placed in boxes of Monte Carlo TIP3P[16] waters such that the smallest distance between any solute atom and a box edge was 12 Å. Any water molecules with a oxygen atom less than 2.40 Å from a solute atom were removed. These restrictions resulted in 593 waters surrounding the 6-Å and 555 waters surrounding the 2-Å structures. Additionally, in order that comparisons between this work and that of Weiner, Singh, and Kollman[9] might be made more readily, the hydro-

Table I. Reaction Energies for Various Ab Inito Basis Sets

calculation	ΔE, kcal mol^{-1}
$HS^- + H_2NCHO \rightarrow HCOS^- + NH_3$[a]	
RHF/STO-3G//RHF/STO-3G	-42.78
RHF/4-31G//RHF/4-31G	-8.60
RHF/6-31G//RHF/6-31G	-0.88
RHF/6-31G*//RHF/6-31G	0.17
RHF/6-31G**//RHF/6-31G	0.16
FMP2-FC/6-31G*//RHF/4-31G	-8.70
FMP2-FC/6-31G*//RHF/6-31G	-7.84
FMP2-FC/6-31G**//RHF/6-31G	-7.47
$HS^- + H^+ \rightarrow H_2S$[b]	
RHF/STO-3G//RHF/STO-3G	505.68
RHF/4-31G//RHF/4-31G	364.16
RHF/6-31G//RHF/6-31G	346.00
RHF/6-31G*//RHF/6-31G	360.02
RHF/6-31G**//RHF/6-31G	362.46
FMP2-FC/6-31G*//RHF/4-31G	362.78
FMP2-FC/6-31G*//RHF/6-31G	362.56
FMP2-FC/6-31G**//RHF/6-31G	368.76
$HCOS^- + H^+ \rightarrow HCOSH$[c]	
RHF/STO-3G//RHF/STO-3G	465.60
RHF/4-31G//RHF/4-31G	339.81
RHF/6-31G//RHF/6-31G	328.62
RHF/6-31G*//RHF/6-31G	342.74
RHF/6-31G**//RHF/6-31G	345.22
FMP2-FC/6-31G*//RHF/4-31G	342.03
FMP2-FC/6-31G*//RHF/6-31G	342.50
FMP2-FC/6-31G**//RHF/6-31G	348.82

[a] Total energy ($HS^-/H_2NCHO/HCOS^-/NH_3$): RHF/STO-3G//RHF/STO-3G, (-393.50578/-166.68821/-504.80674/-55.45542); RHF/4-31G//RHF/4-31G, (-397.62363/-168.68152/-510.21216/-56.10669); RHF/6-31G//RHF/6-31G, (-398.07616/-168.85501/-510.76705/-56.16552); RHF/6-31G*//RHF/6-31G, (-398.09269/-168.92930/-510.84252/-56.17921); RHF/6-31G**//RHF/6-31G, (-398.09658/-168.93908/-510.84412/-56.19129); FMP2-FC/6-31G*//RHF/4-31G, (-398.20993/-169.39290/-511.26824/-56.34846); FMP2-FC/6-31G*//RHF/6-31G, (-398.21022/-169.39315/-511.26767/-56.34818); FMP2-FC/6-31G**//RHF/6-31G, (-398.22156/-169.42021/-511.27600/-56.37769) hartrees. [b] Total energy (HS^-/H_2S): RHF/STO-3G//RHF/STO-3G, (-393.50578/-394.31163); RHF/4-31G//RHF/4-31G, (-397.62363/-398.20395); RHF/6-31G//RHF/6-31G, (-398.07616/-398.62755); RHF/6-31G*//RHF/6-31G, (-398.09269/-398.66642); RHF/6-31G**//RHF/6-31G, (-398.09688/-398.67420); FMP2-FC/6-31G*//RHF/4-31G, (-398.20993/-398.78805); FMP2-FC/6-31G*//RHF/6-31G, (-398.21022/-398.78798); FMP2-FC/6-31G**//RHF/6-31G, (-398.22156/-398.80922) hartrees. [c] Total energy ($HCOS^-$/HCOSH): RHF/STO-3G//RHF/STO-3G, (-504.80674/-505.54872); RHF/4-31G//RHF/4-31G, (-510.21216/-510.75368); RHF/6-31G//RHF/6-31G, (-510.76705/-511.29074); RHF/6-31G*//RHF/6-31G, (-510.84252/-511.38871); RHF/6-31G**//RHF/6-31G, (-510.84412/-511.39426); FMP2-FC/6-31G*//RHF/4-31G, (-511.26824/-511.81330); FMP2-FC/6-31G*//RHF/6-31G, (-511.26767/-511.81349); FMP2-FC/6-31G**//RHF/6-31G, (-511.27600/-511.83187) hartrees.

(11) Binkley, J. S.; Frisch, M. J.; DeFrees, D. J.; Rahgavachari, K.; Whiteside, R. A.; Schlegel, H. B.; Fluder, E. M.; Pople, J. A. *GAUSSIAN 82*; Department of Chemistry, Carnegie Mellon University, Pittsburgh, PA, 1982.

(12) (a) Ammonia, formaldehyde, formamide, hydrogen sulfide, water: Harmony, M. D.; Laurie, V. W.; Kuczkowski, R. L.; Schwendeman, R. H.; Ramsey, D. A.; Lovas, F. J.; Lafferty, W. J.; Maki, A. G. *J. Phys. Chem. Ref. Data* **1979**, *8*, 619. (b) Thioformic acid: Hocking, W. H.; Winnewisser, G. *J. Chem. Soc., Chem. Commun.* **1975**, 63.

(13) Bartmess, J. E.; McIver, R. T., Jr. In *Gas Phase Ion Chemistry*; Bowers, M. T., Ed.; Academic: New York, 1979; Vol. 2, pp 87–121.

(14) Kebarle, P. *Annu. Rev. Phys. Chem.* **1977**, *28*, 445.

(15) (a) Weiner, S. J.; Kollman, P. A.; Case, D. A.; Singh, U. C.; Ghio, C.; Alagona, G.; Profeta, S.; Weiner, P. *J. Am. Chem. Soc.* **1984**, *106*, 765. (b) Singh, U. C.; Weiner, P. K.; Caldwell, J.; Kollman, P. A. *AMBER 3.0*; University of California—San Francisco, 1986.

(16) Jorgensen, W.; Chandresekhar, J.; Madura, J.; Impey, R.; Klein, M. *J. Chem. Phys.* **1983**, *79*, 926.

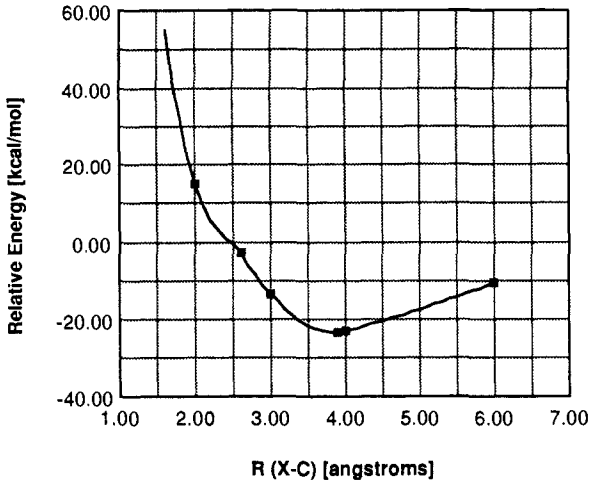

Figure 1. Gas-phase reaction coordinate for hydrosulfide ion + formamide. The curve was constructed by using a cubic spline interpolation of the calculated ab initio energies. The HS^-/H_2NCHO reaction coordinate was calculated at the FMP2-FC/6-31G*//RHF/4-31G level.

sulfide anion in the 6-Å structure was distorted from its original near-coplanar position with respect to formamide to a position such that the HSCN dihedral angle was 0° and the NCS and CSH angles were 90 and 99°, respectively.

The force field equation for AMBER is given by eq 3. Solvent mole-

$$E_{total} = \sum_{bonds} \frac{K_r}{2}(r - r_{eq})^2 + \sum_{angles} \frac{K_\theta}{2}(\theta - \theta_{eq})^2 + \sum_{dihedrals} \sum_{n} \frac{V_n}{2}[1 + \cos(n\phi - \gamma)] + \sum_{i<j} \left(\frac{A_{ij}}{R_{ij}^{12}} - \frac{B_{ij}}{R_{ij}^{6}} \right) + \sum_{\substack{i<j \\ 1\text{-}4\ terms}} \left[\tfrac{1}{2} \left(\frac{A_{ij}}{R_{ij}^{12}} - \frac{B_{ij}}{R_{ij}^{6}} \right) \right] + \sum_{H\text{-}bonds} \left(\frac{C_{ij}}{R_{ij}^{12}} - \frac{D_{ij}}{R_{ij}^{10}} \right) + \sum_{i<j} \left(\frac{q_i q_j}{\epsilon R_{ij}} \right) + \sum_{\substack{i<j \\ 1\text{-}4\ terms}} \left[\tfrac{1}{2} \left(\frac{q_i q_j}{\epsilon R_{ij}} \right) \right] \quad (3)$$

cules were minimized in accordance with this equation by using a "belly" optimization, that is, the solute structures were not allowed to change during the course of the minimization. The molecular mechanical minimizations were continued until the root mean square gradient was less than 0.01 kcal $Å^{-1}$. A nonbonded van der Waals cutoff of 8 Å was used during the calculations, and the hydrogen-bond cutoff was 4 Å. The solute charges were calculated from the electrostatic potential,[17] and a constant dielectric equal to 1 was applied.

The TIP3P waters had oxygen–hydrogen and hydrogen–hydrogen bond force constants of 400 kcal $Å^2$. The waters had an oxygen charge of −0.834 and hydrogen charges of 0.417. All water–water and water–solute hydrogen-bonding interactions were set equal to zero. The water oxygen 6–12 van der Waals radius and well depth were equal to 1.77 Å and 0.16 kcal mol^{-1}, respectively, while these values were zero for the hydrogen atoms.

We were interested in evaluating the solute–solvent and solvent–solvent energy contributions for the two supermolecules. After energy minimization, the waters within ~4 Å of the solute sulfur or oxygen appeared to be those that interacted most strongly with the solute. These waters were thus used during the energy analysis. There were 19 water molecules within 4.00 Å of the solute oxygen or sulfur atoms in the case of the "6-Å" complex. The corresponding distance at which the solvent coordination number reached 19 was 4.10 Å for the "2-Å" structure. We note that this procedure is analogous to that used by Weiner et al.[9] for qualitative estimation of the solvent–solvent energy changes.

Results

There were no notable discrepancies between the experimental structures[12] for the reactants and products depicted in Scheme II and the results of the ab initio geometry optimizations. The reaction coordinate was therefore determined by releasing all degrees of freedom except the sulfur–carbon distance during geometry optimizations of the reactants. We specifically focused on those complexes having sulfur–carbon distances of 6.00, 4.00, 3.00, 2.68, 2.63, 2.00, and 1.50 Å.

Table II. Relative Ab Initio Energies for the Reaction SH^- + $H_2NCHO \rightarrow [H_2N(HS)CHO^-]$

supermolr complex S–C, Å	kcal mol^{-1}		
	E^a	E^b	E^c
∞	0.00	0.00	0.00
6.00	−11.17	−10.20	−10.59
4.00	−27.05	−18.64	−22.86
3.87	−27.95	−19.24	−23.29
3.00	−18.55	−8.98	−13.49
2.68	−8.10	−0.53	−5.19
2.63	−6.18	1.23	−3.66
2.00	21.22	29.04	15.11
1.50	89.66	84.93	67.04

[a] Energy from RHF/4-31G//RHF/4-31G calculation. Absolute energies: ∞ Å, −566.30522; 6.00 Å, −566.32302; 4.00 Å, −566.34833; 3.87 Å, −566.34976; 3.00 Å, −566.33478; 2.68 Å, −566.31813; 2.63 Å, −566.31506; 2.00 Å, −566.27140; 1.50 Å, −566.16234 hartrees. [b] Energy from RHF/6-31G*//RHF/4-31G calculation. Absolute energies: ∞ Å, −567.02245; 6.00 Å, −567.03870; 4.00 Å, −567.05215; 3.87 Å, −567.05311; 3.00 Å, −567.03676; 2.68 Å, −567.02329; 2.63 Å, −567.02049; 2.00 Å, −566.97616; 1.50 Å −566.88710 hartrees. [c] Energy from FMP2-FC/6-31G*//RHF/4-31G calculation. Absolute energies: ∞ Å, −567.60319; 6.00 Å, −567.62007; 4.00 Å, −567.63962; 3.87 Å, −576.64030; 3.00 Å, −567.62469; 2.68 Å, −567.61146; 2.63 Å, −567.60901; 2.00 Å, −567.57911; 1.50 Å, −567.49635 hartrees.

The relative and total energies for the complexes are given in Table II. The overall reaction profile, depicted in Figure 1, appears surprisingly different from that of the analogous hydroxide–formamide reaction.[9] The difference at a reaction coordinate of 6 Å is also large, but this difference between the two reactions is not significant. As noted by Weiner et al.[9], unrestrained geometry optimization at R_{C-O} = 6 Å leads to the reaction $OH^- + H_2NCHO \rightarrow H_2O + HNCHO^-$. Thus, Weiner et al.[9] did not not optimize that particular point on the reaction coordinate of the hydroxide–formamide complex, but kept the $HO^-_{(hydroxide)}$–$NC_{(formamide)}$ dihedral angle at approximately zero degrees. In an ion–dipole interaction (eq 4), the coulomb force

$$V(R,\theta) = \mu Q \cos\theta / 4\pi\epsilon_0 R^2 \quad (4)$$

on the dipole is a function of θ, the angle between the dipole moment vector (μ) and the distance (R) from the center of the dipole to the charge (Q). Since the angle θ was ~90° in the case of the OH^-–formamide complex, the ion–dipole interaction energy would be expected to be close to zero. However, for the SH^-–formamide complex at R_{C-S} = 6 Å, the SH^- moved to the molecular plane and interacted favorable with the NH_2 group. Thus, θ was close to zero, and we would consequently expect a large interaction energy. We have repeated the calculations of Weiner et al.[9] using the 4-31G optimized geometries of the reactants placed in the configuration seen for the SH^-–formamide complex. The interaction energy for the OH^-–formamide complex was calculated to be −10.09 kcal mol^{-1} at the FMP2-FC/6-31G*//RHF/4-31G basis set level, in good agreement with the calculated interaction energy of −10.59 kcal mol^{-1}, which we found for the SH^-–formamide complex at the same basis set level.

A gradual decrease in energy occurs as the sulfur–carbon distance is reduced from infinity to ~4 Å. The energy subsequently steadily increases as the sulfur–carbon distance is further reduced. During the process of decreasing the sulfur–carbon interatomic distance, the hydrosulfide anion migrates from its original near-coplanar arrangement relative to the nitrogen, carbon, and oxygen atoms of formamide to a position above the carbon atom with an orientation that favors minimal overlap with the nitrogen atom orbitals while maintaining maximum bonding overlap with the carbonyl π^*_{CO} orbital. At the same time, the amide group inverts and the carbon atom rehybridizes toward a sp^3 geometry. This geometry has the nitrogen lone pairs oriented trans to the forming C–S bond, which one would expect to be the lowest energy conformer (see Figure 3).

(17) Singh, U. C.; Kollman, P. A. *J. Comput. Chem.* **1984**, *5*, 129.

Table III. Relative Ab Inito Energies for the Reactions HO^- + HCHO → $[HOCH_2O^-]$ and HS^- + HCHO → $[HSCH_2O^-]$

supermolr complex X–C, Å	E, kcal mol^{-1}	supermolr complex X–C, Å	E, kcal mol^{-1}
	HO^- + HCHO → $[HOCH_2O^-]^a$		
∞	0.00	1.80	−44.56
3.00	−23.32	1.60	−51.01
2.50	−26.68	1.51	−52.06
2.00	−37.73	1.40	−48.90
	HS^- + HCHO → $[HSCH_2O^-]^b$		
∞	0.00	2.50	−11.34
4.00	−13.60	2.00	0.59
3.38	−17.16	1.80	15.67
3.00	−14.75		

[a] Energy from RHF/4-31G//RHF/4-31G calculation. Absolute energies: ∞ Å, −188.92240; 3.00 Å, −188.95956; 2.50 Å, −188.96493; 2.00 Å, −188.98253; 1.80 Å, −188.99342; 1.60 Å, −189.00369; 1.51 Å, −189.00537; 1.40 Å, −189.00034 hartrees. [b] Energy from RHF/4-31G//RHF/4-31G calculation. Absolute energies: ∞ Å, −511.31624; 4.00 Å, −511.33792; 3.38 Å, −511.34358; 3.00 Å, −511.33976; 2.50 Å, −511.33432; 2.00 Å, −511.31530; 1.80 Å, −511.29128 hartrees.

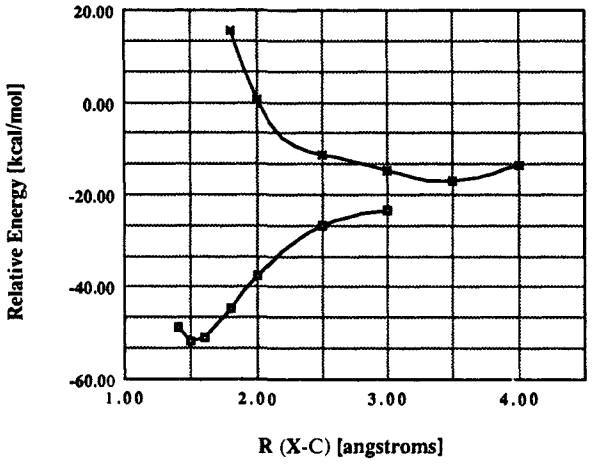

Figure 2. Gas-phase reaction coordinates for hydroxide ion + formaldehyde (lower curve) and hydrosulfide ion + formaldehyde (upper curve). The curves were constructed by using a cubic spline interpolation of the calculated ab initio points. Both reaction coordinates were calculated at the RHF/4-31G//RHF/4-31G ab initio level.

Once the geometry of the 1.50-Å reaction profile point had been established by calculation, the sulfur–carbon constraint was released. The geometry did not relax toward the originally anticipated tetrahedral intermediates but rather converged to an ion–molecule complex. The ion–molecule complex had a sulfur–carbon distance of 3.87 Å and is responsible for the minimum seen in the reaction profile. Its energy was 23.3 kcal mol^{-1} more stable than that of the separated reactants. Several more such calculations were done after altering the HSCN dihedral angle, and in each case, the complex relaxed toward the ion–molecule complex. We then imposed tetrahedral constraints about the carbon atom and optimized the geometries of complexes having sulfur–carbon distances of 2.00, 1.90, 1.80, and 1.70 Å. The energies of these complexes reflected the previously calculated reaction profile, and no undulations in the profile were seen. The reaction coordinate between 3 and 2 Å was also carefully examined for possible local minimum structures. However, no structure was seen in this region at the theoretical levels we utilized.

The unique reaction coordinate for the hydrosulfide–formamide reaction stimulated us to examine the corresponding coordinates for hydroxide and hydrosulfide nucleophilic attack on formaldehyde. The results of these calculations, with formaldehyde constrained to C_s symmetry, are given in Table III and Figure 2. The overall reaction profile and the geometries of the hydroxide–formaldehyde complexes are similar to those which were previously found.[10] We do note several conspicuous differences in our calculational results and those of Madura and Jorgensen[10] which are almost certainly a result of the smaller basis set we utilized for the calculations. We find the $oxygen_{(hydroxide)}$–$carbon_{(formaldehyde)}$ distance to be 1.52 Å in the tetrahedral intermediate instead of the distance of 1.47 Å.[10] In addition, our calculations provided no evidence for the presence of any barrier to the formation of the intermediate. The barrier found by Madura and Jorgensen[10] was very small and involved a transition from the ion–dipole minimum to the tetrahedral intermediate.

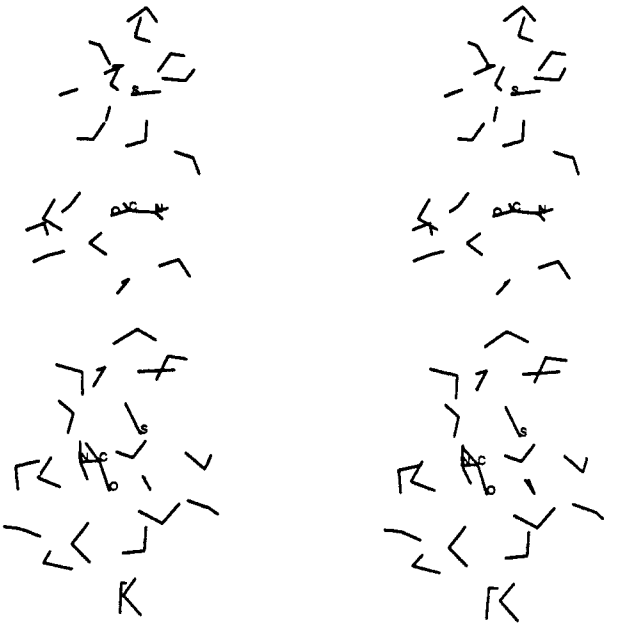

Figure 3. Stereoviews of the hydrosulfide ion/formamide complexes having S–C distances of 6 (upper figure) and 2 (lower figure) Å. Both complexes are shown with a solvent coordination number of 19.

As was noted by Weiner et al.,[9] the need for diffuse basis functions in ab initio calculations is critical for the accurate representation of the relative stabilities of localized (hydroxide) and more delocalized (formate anion and tetrahedral adduct) species. This is the reason for a difference in well depth of the hydroxide–formaldehyde tetrahedral adduct found here (−52 kcal mol^{-1}) and the −35 kcal mol^{-1} well depth reported by Madura and Jorgensen.[10] Clark et al.[18] have shown that the use of diffuse functions also enables a more accurate proton affinity of hydroxide to be calculated, whereas, as mentioned previously, our models without such functions overestimate the proton affinity of hydrosulfide by ~10 kcal mol^{-1}. Nonetheless, we have not employed such functions for two reasons: these functions can cause larger counterpoise errors[19] than comparable "localized" basis sets, and if anything, one would expect the addition of such functions during the calculation of the reaction shown in Scheme II to stabilize the hydrosulfide anion more than the tetrahedral adduct. Thus, the instability of the adduct relative to the reactants would only be increased with such functions.

The shape of the hydrosulfide–formaldehyde reaction profile is comparable to the profile when formamide is the substrate. The only structure seen on the reaction profile is that of a ion–molecule complex. The sulfur–carbon distance in this complex was found to be 3.38 Å, and its energy was 17.2 kcal mol^{-1} more stable than the separated reactants when calculated at the 4-31G level. As in the case of the formamide substrate, imposing tetrahedral constraints on the carbon atom prior to geometry optimization did not reveal any additional structure.

Molecular mechanical calculations, analogous to those used by Weiner et al.,[9] enabled us to obtain an estimate of the relative solvation energies of hydrosulfide and formamide at 6 Å and an adduct with the sulfur–carbon disttance at 2 Å (Figure 3). The relative solute–solvent and solvent–solvent energies of these

(18) Clark, T.; Chandrasekhar, J.; Spitznagel, G.; Schleyer, P. *J. Comput. Chem.* **1983**, *4*, 294.

(19) (a) van Lenthe, J. H.; van Duijneveldt, F. B. *J. Chem. Phys.* **1984**, *81*, 3168. (b) Boys, S. F.; Bernardi, F. *Mol. Phys.* **1970**, *19*, 553.

Table IV. Molecular Mechanics Calculations of Solvation Energies

complex[a] (R_{S-C})	$E_{solute-solvent}$[b]	ΔE solvent–solvent[c]	ΔE solvation[d]	ΔE MM[e]	$\Delta\Delta E_{solvation}$[f]
6.00	−200.0	121.8	−78.3	0.0	0.0
2.00	−154.6	95.4	−59.2	44.7 (34.1)	19.0

[a] Sulfur–carbon distance (Å) in solvated supermolecular complexes. [b] Molecular mechanics nonbonded energy for solute–solvent interactions (kcal mol^{-1}). [c] Molecular mechanics energy difference (kcal mol^{-1}) between the 19 water molecules that interact most strongly with the solute and 19 "ideal" water molecules. The interaction energy of an ideal water is −24.2 kcal mol^{-1}.[9] [d] $E_{solute-solvent} + \Delta E_{solvent-solvent}$ (kcal mol^{-1}). [e] Relative $E_{solute:FMP2-FC/6-31G*//RHF/4-31G} + E_{solute-solvent:MM}$ (kcal mol^{-1}) + $E_{solvent-solvent:MM}$ (kcal mol^{-1}). The value in parentheses was calculated by using the infinitely separated reactants or assuming an attack perpendicular to the amide plane, since the 10.6 kcal mol^{-1} attraction of the ion–dipole complex at 6 Å is unlikely to be important[10] in solution. [f] $\Delta\Delta E_{solvation}$ relative to the reactants (kcal mol^{-1}).

structures are presented in Table IV. The data of particular interest are the $\Delta E_{solvation}$ values of 0 and 19 kcal mol^{-1} for the hydrosulfide–formamide complexes with S–C bond lengths of 6.00 and 2.00 Å, respectively. As one can see, solvation appears to qualtitatively stabilize the reactants over the tetrahedral adduct, but by much less than the 42 kcal mol^{-1} found in the hydroxide–formamide reaction.[9] This is a reasonable result since one might expect hydrogen bonding to be very important to the hydroxide anion due to its highly concentrated charge. The charge distribution difference between the hydrosulfide anion and formamide molecules versus their 2-Å tetrahedral complex would be less dramatic, and thus one would expect a smaller difference in their relative solvation energies. Nonetheless, both intrinsic bonding effects (gas-phase energies) and solvation work against the formation of the hydrosulfide tetrahedral adduct of Scheme II. A qualitative estimate of the stability of this tetrahedral intermediate (Table IV) suggests that it is ~34 kcal mol^{-1} less stable than the reactants, in contrast to Weiner et al.'s estimate of ~16 kcal mol^{-1} for the corresponding hydroxide ion case.

Discussion and Conclusions

We have found the gas-phase reaction coordinate for the nucleophilic attack of hydrosulfide ion on formamide to be both unusual and distinguished by the absence of a stabilizing potential for a tetrahedral complex. This contrasts with what was found[9] for the analogous hydroxide–formamide reaction in which a stable tetrahedral complex was identified. It is clear that the results we have found cannot be simply a consequence of the nature of the substrate since the hydrosulfide–formaldehyde reaction coordinate displays the same features. The origin of the dramatic difference between the hydroxide and hydrosulfide adducts is most certainly related to the difference in C–O and C–S bond strengths. The additional uncertainty concerning the role of charge delocalization of anions in the gas phase precludes a quantitative analysis of these factors, but a rudimentary calculation[20] indicates that the hydroxide ion reaction would be exothermic by ~13 kcal mol^{-1} while the reaction with the hydrosulfide ion would require ~12 kcal mol^{-1} of energy to proceed.

We must stress that the quantum mechanical models used to estimate the relative energies of the hydrosulfide and formamide reactants and their tetrahedral adduct are only at a modest level of accuracy with respect to basis set and correlation corrections. Nonetheless, as noted above, any errors in the model are likely to underestimate the stabilization of the reactants relative to the tetrahedral adduct. Thus, our qualitative result indicating significant destabilization of the tetrahedral adduct relative to the reactants, in contrast to the corresponding hydroxide ion reaction, is almost certainly correct.

In addition, our molecular mechanical model to estimate relative solvation energies is very simple and is inferior to that employed by Madura and Jorgensen.[10] Nevertheless, the stabilization of the reactants relative to the products and the fact that the magnitude of this stabilization is significantly smaller for the hydroxide nucleophile as opposed to the hydrosulfide nucleophile are reasonable results and unlikely to be qualitatively altered by more sophisticated calculations.

Scheme III

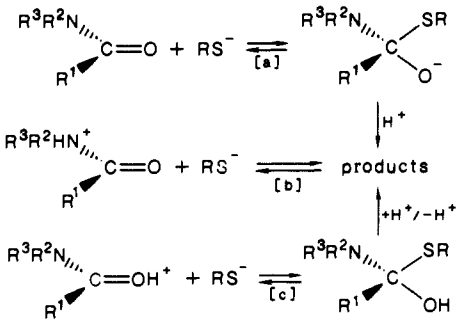

Table V. Relative Energies for Acid-Catalyzed Nucleophilic Addition Reactions

calculation	ΔE kcal mol^{-1}
$HS^- + H_2COH^+ \rightarrow H_2C(SH)OH$[a]	
FMP2-FC/6-31G*//RHF/4-31G	−122.47
$HS^- + H_2NC(H)OH^+ \rightarrow H_2NC(H)(SH)OH$[b]	
RHF/4-31G//RHF/4-31G (no constraints)	−144.73
RHF/4-31G//RHF/4-31G (R_{C-S} = 1.96 Å)	−144.73
RHF/4-31G//RHF/4-31G (R_{C-S} = 2.16 Å)	−141.70
RHF/4-31G//RHF/4-31G (R_{C-S} = 2.50 Å)	−131.06
FMP2-FC/6-31G*//RHF/4-31G	−146.52
$HS^- + H_3N^+C(H)O \rightarrow H_3N\cdots H(HS)CO$[c]	
FMP2-FC/6-31G*//RHF/4-31G	−165.56

[a] Total energy [$HS^-/H_2COH^+/H_2C(SH)OH$]: FMP2-FC/6-31G*//RHF/4-31G, (−398.20993/−114.40470/−512.80980) hartrees. [b] Total energy [$HS^-/H_2NC(H)OH/H_2NC(H)(SH)OH$]: RHF/4-31G//RHF/4-31G (no constraints), (−397.62363/−169.01844/−566.87272); RHF/4-31G//RHF/4-31G (R_{C-S} = 1.96 Å), (−397.62363/−169.01844/−566.87272); RHF/4-31G//RHF/4-31G (R_{C-S} = 2.16 Å), (−397.62363/−169.01844/−566.86788); RHF/4-31G//RHF/4-31G (R_{C-S} = 2.50 Å), (−397.62363/−169.01844/−566.85093); FMP2-FC/6-31G*//RHF/4-31G, (−398.20993/−169.71748/−568.16090) hartrees. [c] Total energy [$HS^-/H_3N^+C(H)O/H3N\cdots H(HS)CO$]: FMP2-FC/6-31G*//RHF/4-31G: [−398.20993/−169.69905/−568.17282]hartrees.

Thiolate ion addition to amides may occur by one of three general mechanisms: (a) initial attack of the carbonyl carbon by the thiolate ion, followed by proton transfer to yield products,[21] (b) N-protonation of the amide and subsequent decomposition of the intermediate tetrahedral adduct, and (c) O-protonation of the amide, followed by attack of the nucleophile and subsequent decomposition to the products[21] (Scheme III). We have shown that a significant barrier exists for mechanism a in both gas and solution phase. If our qualitative estimates are correct, it would cost ~34 kcal mol^{-1} [15 kcal mol^{-1} (gas phase) plus 19 kcal mol^{-1} (solvation)] to form the tetrahedral adduct via mechanism a. Thus, one might pay the energetic price of protonating the amide group, in which case the hydrosulfide ion attack could proceed by mechanism b or c with no *intrinsic* barrier.

In order to test the reasonableness of this proposal, we have performed ab initio calculations on the O-protonated formaldehyde substrate, the O- and N-protonated formamide substrates, and their tetrahedral adducts with the hydrosulfide anion. The compounds were geometry optimized at the 4-31G level and single-point energies were obtained at the 4-31G, 6-31G*, and MP2/6-31G* levels. These results are summarized in Table V.

In contrast to the uncatalyzed reaction, HS^- forms a stable tetrahedral intermediate with H_2COH^+, and its energy at the MP2/6-31G* level is calculated to be ~122 kcal mol^{-1} more stable

(20) Bond strengths S–C, 66.36 kcal mol^{-1}; O–C, 90.99 kcal mol^{-1}: Lovering, E. G.; Laidler, K. J. *Can. J. Chem.* **1960**, *38*, 2367. C=O, 169 kcal-mol^{-1}: Berry, R. S.; Rice, S. A.; Ross, J. *Physical Chemistry Part 2 [Matter in Equilibrium: Statistical Mechanics and Thermodynamics]*; Wiley: New York, 1980, pg 564.

(21) Fersht, A. R. *J. Am. Chem. Soc.* **1971**, *93*, 3504.

than the reactants. The S-C bond length was calculated to be 1.91 Å for the tetrahedral intermediate. The O-protonated formamide was found to be 24.5 kcal mol^{-1} more stable than the N-protonated species at the MP2/6-31G* level of calculation. No stable tetrahedral intermediate was found for the N-protonated formamide–HS^- reaction; rather, the NH_3 was such a good leaving group that geometry optimization of tetrahedral H3N-C(H)-(SH)O immediately led to the formation of a stable hydrogen-bonded complex of H_3N-HSCHO. This is analogous to the study of water-catalyzed proton transfer in the tetrahedral intermediate of HO^-/formamide by Weiner et al.[9], in which, as soon as the water proton had migrated to the NH_2 group, the C-N bond spontaneously lengthened. Finally, the reaction of the O-protonated formamide with HS^- led to a stable tetrahedral intermediate with a MP2/6-31G* energy that was 146 kcal mol^{-1} more stable than the reactants. The S-C bond length of this intermediate was 1.96 Å. In addition, geometry optimizations with S-C constraints of 1.96, 2.16, and 2.50 Å showed a smooth potential and did not detect any barrier to the formation of this intermediate.

It is generally agreed[22] that protonation of amides occurs preferentially at the oxygen, not nitrogen, atom. The above results, in conjunction with the previously mentioned results for the unprotonated carbonyl compounds, are consistent with a mechanism in which O-protonation of the carbonyl substrate precedes or accompanies attack by the hydrosulfide anion during a nucleophilic addition. The above considerations lead us to speculate that in the thiol protease enzyme papain, where it appears that the active site sulfhydryl is anionic and the histidine cationic,[23] the sulfhydryl attack may be preceded or accompanied by proton transfer from the imidazole ring of histidine-159 (His) to the substrate rather than following it, as appears to be the case in the serine proteases. Based on the pK_a of an amide group, preprotonation of the substrate in papain is more likely on the oxygen, but it is not clear if His can accomplish this or if there is an alternative acid. Preprotonation of the oxygen would make an "oxy anion hole"—with NH groups pointing toward the carbonyl group—an unfavorable structural element. Alternatively, protonation of the amide nitrogen, unfavorable per se, might be possible if the enzyme distorts the amide group from planarity[24] or if protonation is accompanied by concerted RS^- attack. Given our energy estimates, mechanism a, attack by RS^- preceding protonation, is the least likely mechanism to describe the reaction.

Acknowledgment. We are pleased to acknowledge research support from the NIH (Grant GM-29072 to P.A.K.) and the use of the UCSF Computer Graphics Laboratory facilities through Grant RR-1081 to R. Langridge. Some of the computer calculations were run on the SDSC Cray XMP and this use was supported by the NSF Grant DMB-84-19883.

Registry No. HS^-, 15035-72-0; H_2NCHO, 75-12-7; HCHO, 50-00-0; HO^-, 14280-30-9; $HCOS^-$, 37619-01-5; H_2COH^+, 18682-95-6; H_2NC-[H]OH^+, 50785-80-3.

(22) Katritzky, A. R.; Jones, R. A. Y. *Chem. Ind. (London)* **1961**, 722.

(23) Lewis, S. D.; Johnson, F. A.; Shafer, J. A. *Biochemistry* **1976**, *15*, 5009.

(24) Johansson, A.; Kollman, P.; Rothenberg, S.; McKelvey, J. *J. Am. Chem. Soc.* **1974**, *96*, 3794.

Lipase-Catalyzed Irreversible Transesterifications Using Enol Esters as Acylating Reagents: Preparative Enantio- and Regioselective Syntheses of Alcohols, Glycerol Derivatives, Sugars, and Organometallics

Yi-Fong Wang, James J. Lalonde, Milagros Momongan, David E. Bergbreiter,* and Chi-Huey Wong*

Contribution from the Department of Chemistry, Texas A&M University, College Station, Texas 77843. *Received November 16, 1987*

Abstract: Isopropenyl and vinyl esters have been found to be useful for lipase-catalyzed stereoselective acylation of a number of hydroxy compounds including glycerol and serinol derivatives, ferrocenylethanol, sugars, and other alcohols. The reactions are faster, more selective, and easier to optimize than other transesterifications using alkyl esters as acylating reagents. The alcohol freed from the transesterification rapidly tautomerizes to volatile acetaldehyde or acetone, making the process *irreversible* and simpler for product isolation. The process is particularly useful for synthesis of certain chiral compounds, such as ferrocenyl ethyl esters and acyl sugars, which are difficult to prepare in aqueous solution. Compared to hydrolysis, transesterifications are about 10^2–10^4 times slower with normal alkyl esters as acylating reagents and about 10 times slower with the enol esters as acylating reagents. In some cases, transesterifications are less selective than hydrolyses.

Hydrolytic enzymes such as lipases, esterases, and proteases have been extensively used as catalysts in enantioselective syntheses.[1] Because of their relatively high stability in organic media, they can also be used in organic solvents for certain types of transformations which are difficult to do in water.[2] The most common reactions are esterase- and lipase-catalyzed stereoselective esterifications and transesterifications.[2-7] The reactions, however,

(1) For reviews in the field, see: Whitesides, G. M.; Wong, C.-H. *Angew. Chem., Int. Ed. Engl.* **1985**, *24*, 617. Jones, J. B. *Tetrahedron* **1986**, *42*, 3351. Roberts, S. M. *Chem. Br.* **1987**, 127. Akiyama, A.; Bednarski, M.; Kim, M. J.; Simon, E. S.; Waldmann, H. I.; Whitesides, G. M. *Ibid.* **1987**, 645.

(2) Klibanov, A. M. *CHEMTECH* **1986**, 354-359. Klibanov, A. M.; Cambou, B. *J. Am. Chem. Soc.* **1984**, *106*, 2687-2692.

(3) Chen, C.-S.; Wu, S.-H.; Girdaukas, G.; Sih, C. J. *J. Am. Chem. Soc.* **1987**, *109*, 2812-2817. Guo, Z. W.; Sih, C. J. *Ibid.* **1988**, *110*, 1999-2001.

(4) Gil, G.; Ferre, E.; Meou, A.; Petit, J. L.; Triantaphylides, C. *Tetrahedron Lett.* **1987**, *28*, 1647 and references cited.

(5) Yokozeki, K.; Yamanaka, S.; Takinami, K.; Hirose, Y.; Tanaka, A.; Sonomoto, K.; Fukui, S. *Eur. J. Appl. Microbiol. Biotechnicol.* **1982**, *14*, 1.

(6) Tambo, G. M. R.; Schar, H.-P.; Busquets, X. F.; Ghisalba, O. *Tetrahedron Lett.* **1986**, *27*, 5705-5710. Belan, A.; Bolte, J.; Fauve, A.; Gourey, J. G.; Veschambre, H. *J. Org. Chem.* **1987**, *52*, 256-260 (The latter is for synthesis of (*S*)-**14a**).

0002-7863/88/1510-7200$01.50/0